Stabilization of charge-density waves in $1T$-TaX_2(X=S,Se,Te): First-principles total energy calculations

S. Sharma and L. Nordström
Condensed Matter Theory Group, Department of Physics, Uppsala University, BOX 530, S-751 21 Uppsala, Sweden

B. Johansson
Condensed Matter Theory Group, Department of Physics, Uppsala University, BOX 530, S-751 21 Uppsala, Sweden and Applied Materials Physics, Department of Materials Science and Engineering, Royal Institute of Technology, SE-100 44 Stockholm, Sweden

(Received 9 February 2002; published 7 November 2002)

The quasi-two-dimensional transition-metal dichalcogenide compounds $1T$-TaX_2(X=S,Se,Te) at low temperature form charge-density waves (CDW), manifested in periodic lattice distortions. In order to investigate the effect of the CDW on the Fermi surface (FS) of these compounds, the FS cross sections in various planes are calculated and the nesting vectors are determined. The CDW is treated as single q commensurate frozen phonons of wave vectors around the candidate FS nesting vectors. The lattice distortions caused by the CDW are then reproduced using the total energy and force calculations performed within these supercells using the full potential linearized augumented plane-wave method. It was found that these compounds are unstable towards the CDW state. Our FS calculations for the CDW distorted state confirm the presence of gaping in the FS indicating that electron-phonon coupling plays an important role in the stabilization of the CDW in the compounds under investigation.

DOI: 10.1103/PhysRevB.66.195101 PACS number(s): 71.18.+y

I. INTRODUCTION

During the past three decades there has been a lot of interest in the structural, optical, electromagnetic, and superconducting properties of transition-metal dichalcogenide (TMDC) layered compounds. These compounds have a formula TX_2, where T is the transition metal of groups IVB, VB, or VIB of the periodic table and X is one of the chalcogens (S, Se, or Te). Structurally these compounds can be regarded as two-dimensional (2D) X-T-X layers or sandwiches with strong and primarily covalent intralayer bonding, while the interlayer bonding is weak and of van der Waals type. The 2D nature of bonding is responsible for a number of unusual physical properties. For example, electrical and thermal conductivity are found to be significantly lower along c axis compared to the basal plane.

The materials we are concerned with here are TaX_2(X=S,Se,Te) in the so-called $1T$ structure. These materials have stimulated ongoing experimental work because of their unique physical properties different from groups IVB and VIB TMDC. Several experiments such as x-ray analysis,[1–4] thermal-conductivity measurements,[5] photoemission spectroscopy,[6–12] high-resolution angle scanned photoemission,[13] and Mössbauer[14] effect have been performed to shed light on the puzzling behavior of these compounds. As the results of weak van der Waals interlayer forces, these compounds can be intercalated with foreign atoms and molecules leading to significant and dramatic changes in their physical properties, which has been studied by doping with cation and anions.[15–18] Single crystals of these compounds usually grow in the form of thin platelets. These can be readily cleaved to produce samples that are only few angstroms thick along c axis. Such samples are amenable to surface-sensitive techniques such as scanning tunneling microscopy (Refs. 19–21) and angle-resolved photoemission spectroscopy (ARPES) experiments.[6–12] Insights gained from these recent experiments have stimulated renewed interest in these compounds.

Several semiempirical band structure and ligand field models have been proposed to describe the electronic states of these compounds. Wilson and Yoffe[22] have discussed a schematic energy band model for several groups of TX_2 compounds. Later Bromley, Murray, and Yoffe[23] applied the tight-binding method to calculate the band structure. Mattheiss used the augmented plane-wave (APW) method to determine the energy bands of $1T$-TaS_2 and other similar compounds,[24] while Myron and Freeman used the Korringa-Kohn-Rostoker method to calculate the band structure and the Fermi surface (FS).[25] More recently, Vernes *et al.* have used a tight-binding linear muffin-tin orbital (TB-LMTO) method to calculate the band structure and FS of $TaTe_2$ (Ref. 26) with $C2/m$ structure, and Sharma *et al.* have used the linear muffin-tin orbital method within atomic sphere approximation (LMTO-ASA) to calculate the band structure and optical properties of these compounds.[27]

Numerous studies of the electronic properties have been carried out, due in particular to the charge-density wave (CDW) phenomena that is encountered in these compounds. Wilson *et al.* were the first to observe the CDW in $1T$-TaS_2.[28] The undistorted phase for $1T$-TaS_2 exists for a very small temperature range above 550 K. Upon cooling, it shows a CDW distortion that is incommensurate with the underlying lattice.[17] The CDW goes from an incommensurate to nearly commensurate phase as the temperature is lowered to 350 K. On further cooling (at 180 K), the existing CDW rotates into an orientation for which it becomes com-

TABLE I. Lattice parameters of $1T$-TaX_2 compounds.

Compound	a(Å)	c/a (Å)	Optimized z
$1T$-TaS_2	3.365	1.751	0.2571
$1T$-$TaSe_2$	3.477	1.804	0.2614
$1T$-$TaTe_2$	3.740	1.800	0.2614

mensurate. The commensurate phase is manifested by a $\sqrt{13}a\times\sqrt{13}a$ structure. $1T$-$TaSe_2$ shows a similar structure at low temperature, but in this case the initial CDW onset occurs at 600 K followed by an incommensurate-to-commensurate transition at 473 K. In both the compounds CDW forms a triple q structure with three equivalent vectors rotated by 120° in the plane of the sandwich, i.e., it is a superposition of three different order parameters corresponding to three independent wave vectors of the same star. The observed low-temperature structure of $1T$-$TaTe_2$ is of single q CDW type, although it is not referred to as a CDW. This is probably due to comparatively large amplitude of the CDW compared to the other two compounds. Considerable work has been done to understand these instabilities, yet the nature behind the CDW formation is clouded with controversy.

Fazekas and Tosatti proposed that a Mott-Hubbard transition occurring at 180 K explains this behavior,[29] which would reflect the importance of electron correlations. Okajima and Tanaka[30] supported this viewpoint. Claessen *et al.*[8] explained the behavior of low-temperature resistivity using Mott localization accompanied by pinning of the Fermi level. More recently, Pillo *et al.*[9,31] performed ARPES experiments to show that this correlation pseudogap in the FS exists even at the room-temperature quasicommensurate CDW phase and the transition from quasicommensurate-to-commensurate CDW phase at low temperature takes place due to Mott localization of Ta $5d$ electrons. DiSalvo and co-workers, on the other hand, argued that the CDW transition was caused by Anderson localization due to impurities and unspecified structural defects.[15,32,33] They studied the resistivity behavior of cation and anion doped $1T$-TaS_2 and $TaSe_2$ to support this argument. Fukuyama and Yosida could within this model explain the low-temperature behavior of magnetoresistance by a theory based on this variable range hopping conduction.[34,35] Fazekas and Tosatti[29] discarded this, arguing that if the electron localizes due to disorder then the resistivity should increase with both cation and anion doping, while it was found to decrease with cation doping. A third mechanism was proposed by Doublet *et al.*[36] From band structure, crystal orbital population, and density-of-state calculations, they concluded that the electron transfer from the chalcogen-chalcogen bonding state to transition metal-chalcogen antibonding state is responsible for formation of the $\sqrt{13}a\times\sqrt{13}a$ structure in $1T$-TaS_2 and $1T$-$TaSe_2$. A widespread point of view is that the FS nesting yields a suitable condition for the CDW distortions[17,28,37] through electron-phonon coupling. The idea is that the system of interacting electrons can stabilize a broken-symmetry ground state like the CDW state. In the CDW state, the so-called ''Peierls gap'' opens up in the energy-level distribution at the Fermi level due to formation of electron-hole pair with the wave vector q_{CDW}, and this dictates a new periodicity in the CDW state.

The controversy regarding the mechanism behind the stabilization of the CDW is not unique to these materials, but rather is a subject of controversy for several materials,[38–42] $1T$-TaS_2 is one of the most studied material because it is one of the first materials in which the CDW was discovered by means of x-ray-diffraction experiments. Also $1T$-TaS_2 goes through several phases before the formation of the $\sqrt{13}a\times\sqrt{13}a$ structure, so the material has become a good test material during the past decade for different kind of experiments and theories to explain the ground state and mechanism of stabilization of the CDW.

In the view of the conflicting arguments for explaining the gaping in the FS at low temperature, there is a need for an accurate electronic structure calculation for the CDW state. We intend to fulfill this requirement by studying the single q commensurate CDW and its effect on the FS of these compounds. There are two reasons for studying single q commensurate CDW, instead of observed triple q. First is that the problem becomes much more physically transparent, it is easier to understand the effect of single q CDW on the FS compared to the triple q CDW and second is that it saves a lot of computer time as the supercell is only of the order three to five times that of the $1T$ cell compared to 13 times for the $3q$ CDW. In addition, the observed low-temperature structure of $1T$-$TaTe_2$ can be viewed as $3a\times1a$, which is single q CDW type.

For all three compounds there is a lack of systematic calculations that could reveal both the FS behavior and the manner in which these compounds change on going from disulphide to ditelluride. In fact, we are not aware of any calculation of the FS of $1T$-$TaTe_2$. In this paper, we present *ab initio* calculations of the FS of all the three compounds.

As in experiments,[17,37] our calculated FS sheets are imperfectly nested. The FS of $TaSe_2$ and $TaTe_2$ changes topology perpendicular to the basal plane. The magnitude of the nesting vector changes along the c axis, so in order to study this change the FS cross sections perpendicular to the basal plane have been plotted. These candidate FS nesting vectors are then used to determine the CDW wave vectors. The CDW is treated as a frozen phonon of wave vector q_{CDW} and the supercell, that best mimics this phonon in one dimension, is then set up. Finally, with the use of total energy and forces, the atomic positions are relaxed in accordance with the CDW. The magnitude of these relaxations might be viewed as the CDW amplitude. We find that CDW distorted structures do stabilize. This leads us to believe that the CDW distortions are indeed mediated by electron-phonon coupling. In the case of $TaSe_2$ and $TaTe_2$, the major portions of the FS vanish due to CDW distortions. However, for TaS_2 even though the superstructure gains energy due to CDW distortion, the amplitude of the CDW is very small and the FS does not show any gaping.

The paper is arranged in the following manner. In Sec. II, we present the details of calculations. Section III A deals with the FS and nesting vectors of the $1T$ phase of all three compounds. We discuss the optimized supercell in Sec. III B.

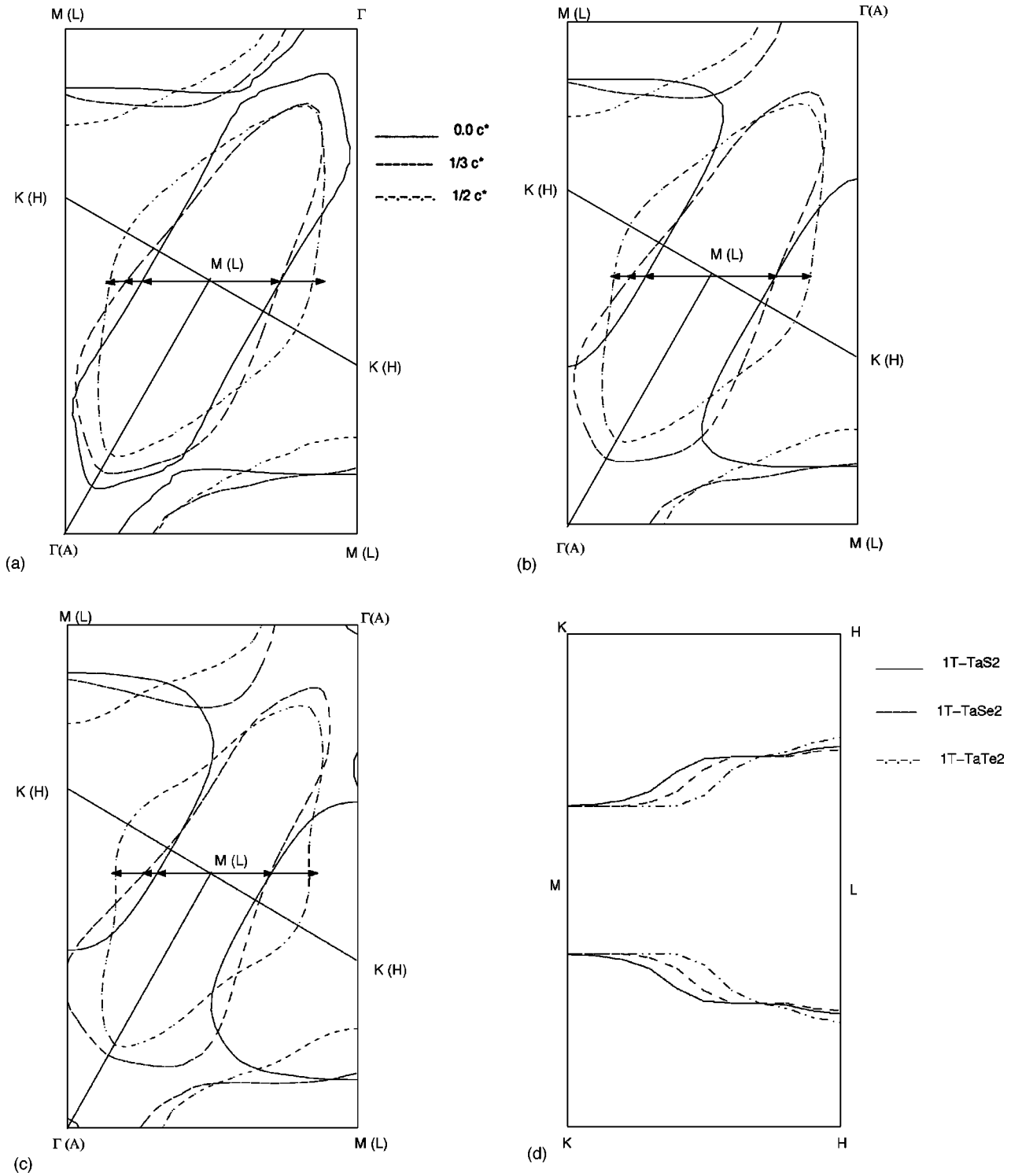

FIG. 1. (a) The Fermi-surface cross sections of $1T$-TaS_2 in the $\Gamma MK\Gamma M$ plane (basal plane), plane at a distance $\frac{1}{3}c^*$ from the basal plane and in the $ALHAL$ plane (at a distance $\frac{1}{2}c^*$ from the basal plane). The arrows show the Fermi-surface nesting vectors (parallel to the ΓM direction) in the various planes. (b) The Fermi-surface cross sections of $1T$-$TaSe_2$ in the $\Gamma MK\Gamma M$ plane (basal plane), plane at a distance $\frac{1}{3}c^*$ from the basal plane and in the $ALHAL$ plane (at a distance $\frac{1}{2}c^*$ from the basal plane). The arrows show the Fermi-surface nesting vectors (parallel to the ΓM direction) in the various planes. (c) The Fermi-surface cross sections of $1T$-$TaTe_2$ in the $\Gamma MK\Gamma M$ plane (basal plane), plane at a distance $\frac{1}{3}c^*$ from the basal plane and in the $ALHAL$ plane (at a distance $\frac{1}{2}c^*$ from the basal plane). The arrows show the Fermi-surface nesting vectors (parallel to the ΓM direction) in the various planes. (d) The Fermi-surface cross sections of $1T$-TaS_2, $1T$-$TaSe_2$, and $1T$-$TaTe_2$ in $KHLHKM$ plane.

TABLE II. The basal plane projected experimental CDW wave vectors, previous calculated FS nesting vectors in the basal plane, and our calculated FS nesting vectors in various planes, in the units $a^* = 4\pi/\sqrt{3}a$

Compound	Distance from the basal plane (plane)	The experimental CDW wave vector q_{CDW}(expt.) (Ref. 17)	The results of Myron and Freeman (Ref. 25)	Our results (q_N)	Our results [$q_N(13.9°)$]
$1T$-TaS_2	0.0 (ΓMK)	0.288	0.34	0.236	0.210
	$\frac{c^*}{3}$			0.264	0.236
	$\frac{c^*}{2}$ (ALH)			0.347	0.333
$1T$-$TaSe_2$	0.0 (ΓMK)	0.285	0.32	0.225	0.201
	$\frac{c^*}{3}$			0.298	0.285
	$\frac{c^*}{2}$(ALH)			0.326	0.329
$1T$-$TaTe_2$	0.0 (ΓMK)	0.333		0.195	
	$\frac{c^*}{3}$			0.215	
	$\frac{c^*}{2}$ (ALH)			0.333	

Section III C includes the FS of the supercells, and finally in Sec. IV we present the summary of our calculations.

II. METHODOLOGY

The compounds under investigation have a hexagonal Bravais lattice. The Ta atom is octahedrally coordinated by the chalcogen atoms(S, Se, or Te), with one sandwich per unit cell (space group $D^3{}_{3d}P_{3m1}$). The Ta atom is located at (0,0,0) and the chalcogen atom at $\pm(1/3,2/3,z)$. There is an ideal value of $z=1/4$, but we have optimized z and then used it for all the calculations. However, we have used the experimental lattice parameters[22] given in Table I.

The full potential linearized augumented plane-wave (FPLAPW) calculations are performed using the WIEN97 code,[43] including the local orbitals for the high-lying ''semicore states.'' The calculations are performed within the local-density approximation (LDA) and the scalar relativistic equations are used to obtain self-consistency. On one hand, it is well known that LDA underestimates the equilibrium bonding distances and, on the other hand, there is a general consensus that the LDA gives a good representation of the electronic structure at the experimental lattice parameters therefore no attempts have been made to optimize the lattice parameters (a and c/a). The self-consistent calculations are performed using 204k points in the irreducible Brillouin zone for the $1T$ structures, and with 183k points in the irreducible Brillouin zone for the supercell. The FS is calculated using a mesh of 3600k points in the plane.

III. RESULTS AND DISCUSSION

A. $1T$-TaX_2(X=S,Se,Te)

First, we shall discuss the importance of the optimization of parameter z. The calculations performed for the ideal z show that there are forces on the chalcogen atoms which cannot be neglected, so the relaxation of the structure is needed. In addition, the band structure for the ideal $1T$-TaS_2 shows that three bands cut the Fermi level, and for $1T$-$TaSe_2$ and $1T$-$TaTe_2$ two bands cut the Fermi level. The FS formed by these bands is much more complicated than the experimental results.[7,9,11,37,44] The bands cutting Fermi level is narrow and so the FS topology is very sensitive to small adjustments in both the shape of the bands and the Fermi energy. On complete relaxation of the structure, there is a gain in energy of 1.09, 5.13, 3.86 mRy/formula unit for TaS_2, $TaSe_2$, and $TaTe_2$, respectively, reflecting the fact that the ideal z structure is unstable. The value of the optimized z for the three compounds is presented in Table I. The band structures for the three compounds with optimized z are much simpler with just one band cutting the Fermi level. In Fig. 1, we present our results for the FS in $\Gamma MK\Gamma M$ plane (basal plane) for all the three compounds. In order to see the variation in the FS perpendicular to the basal plane, Fig. 1 includes the FS cross sections in the planes parallel to the basal plane and at a distance $c^*/3$ and $c^*/2$ ($ALHAL$ plane) from it.

The FS of $1T$-TaS_2 [Fig. 1(a)] is a closed electron sheet around M and shows variation parallel to the basal plane along the c axis. The FS of $1T$-$TaSe_2$ [Fig. 1(b)] comprises a closed electron sheet around K. The FS changes topology on moving up from the basal plane along the c axis, and at a distance of $c^*/5$ from the basal plane it becomes a closed electron sheet around the point above M. These results are in accordance with recent band-structure calculations.[37] The calculated FS of $1T$-$TaTe_2$ is a closed electron sheet around K in the basal plane [Fig. 1(c)]. Like the FS of $TaSe_2$, it changes topology and becomes a closed electron sheet around the point above M at a distance of $c^*/4.4$ from the basal plane.

As is clear from the FS topology, several portions of the FS can be nested by choosing different sets of spanning vec-

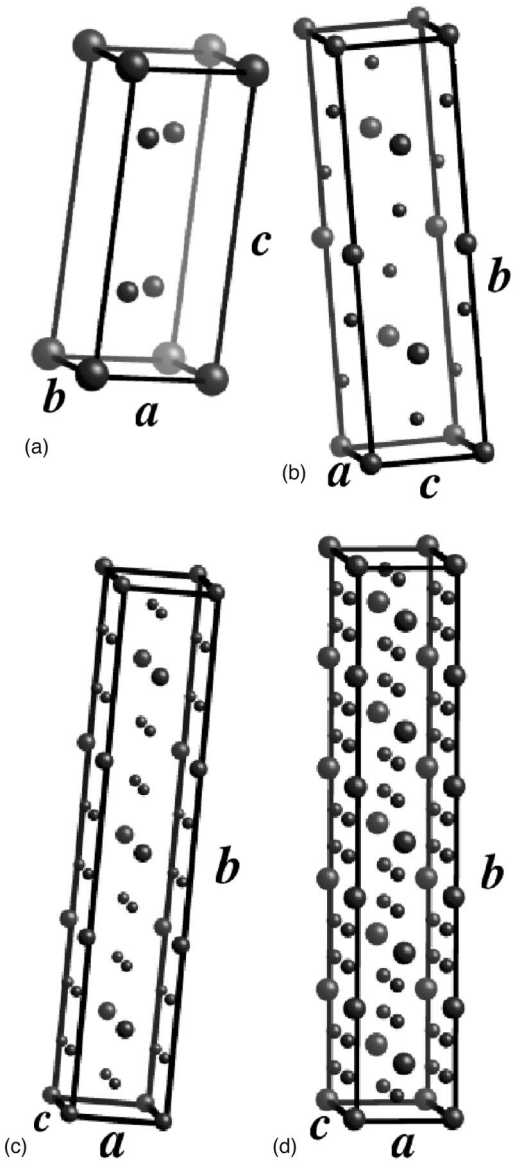

FIG. 2. (a) The unit cell for $1T$-TaX_2 compounds. The big spheres are the Ta atoms and the small sphere are the chalcogen atoms. (b) The supercell corresponding to $q_{CDW}=0.333a^*$. The big spheres are the Ta atoms and the small sphere are the chalcogen atoms. (c) The supercell corresponding to $q_{CDW}=0.250a^*$. The big spheres are the Ta atoms and the small sphere are the chalcogen atoms. (d) The supercell corresponding to $q_{CDW}=0.200a^*$. The big spheres are the Ta atoms and the small sphere are the chalcogen atoms.

tors. The most favorable nesting vectors (q_N) are parallel to ΓM for all the compounds studied in this work. We compare our calculated nesting vectors in the units of $a^*(a^*=4\pi/\sqrt{3}a)$ to the previous calculations[25] and to the experimental results of CDW wave vector $[q_{CDW}(\text{expt.})]$ parallel to the ΓM direction[17] in Table II. The experimental CDW wave vectors for $TaSe_2$ and TaS_2 listed in Table II are the basal plane projected wave vectors of the triple q CDW, which are incommensurate with the underlying lattice. Wilson *et al.* found that the value of q_{CDW}(expt.) becomes

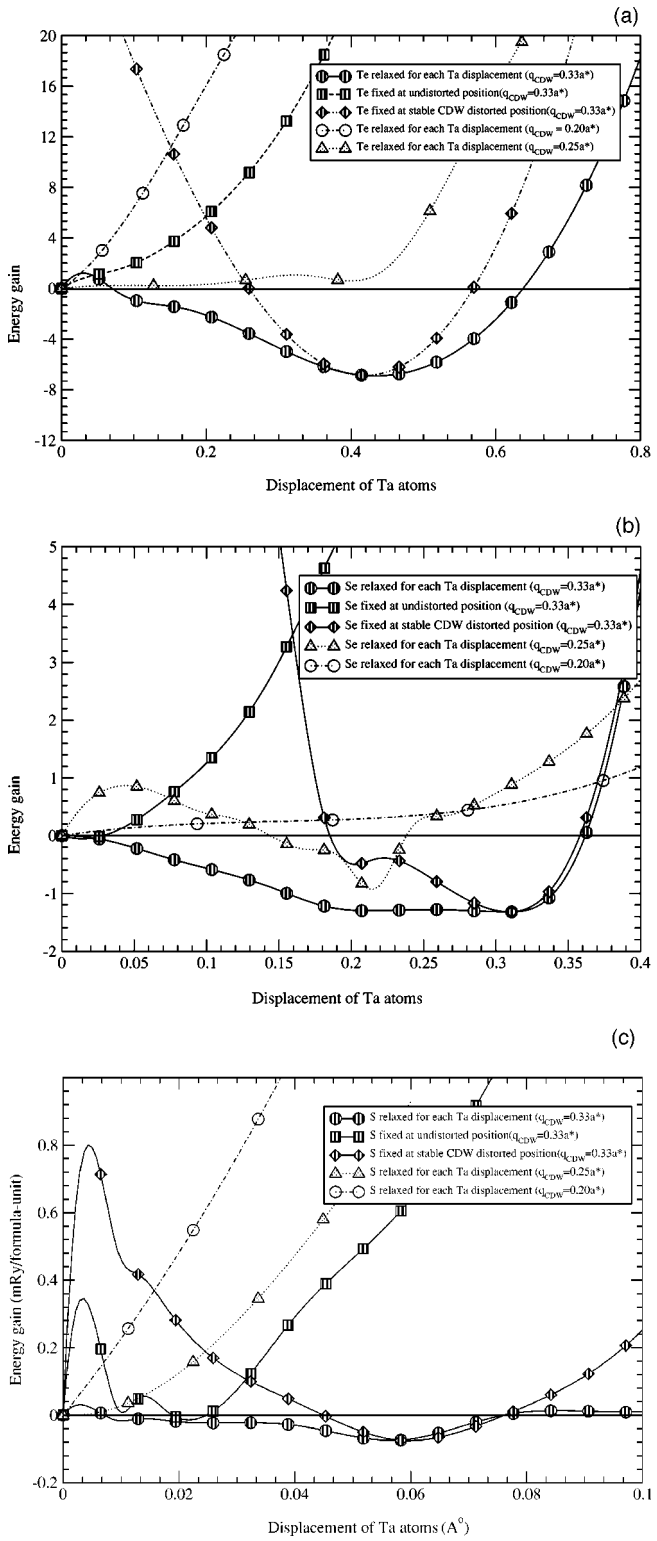

FIG. 3. (a) The gain in energy relative to the undistorted supercell vs the displacement of the Ta atoms in $TaTe_2$. (b) The gain in energy relative to the undistorted super cell vs the displacement of the Ta atoms in $TaSe_2$. (c) The gain in energy relative to the undistorted supercell vs the displacement of the Ta atoms in TaS_2.

$(1/\sqrt{13})a^*$ for $TaSe_2$ and close to this for TaS_2 when the CDW at low temperatures becomes commensurate by rotating by an angle of 13.9°. It is also therefore interesting to

look at the magnitude of the vector that nests the FS at an angle of 13.9° to the ΓM direction. This is denoted by $q_N(13.9°)$ in the table. Pillo *et al.*[31] have calculated this value for $1T$-TaS_2 to be equal to $0.277a^*$. For $TaTe_2$ the q_{CDW}(expt.) is the wave vector of single q commensurate CDW.

Since the FS of $TaSe_2$ and $TaTe_2$ changes topology with the variation in the vector perpendicular to the basal plane, so we have listed the nesting vectors parallel to the ΓM direction at distances $c^*/3$ and $c^*/2$ from the basal plane.

In Fig. 1(d), we plot cross sections of the FS of the three compounds in $KHLHKM$ plane. Looking at this two things becomes clear. First is that there are several possible nesting vectors of different magnitude in the phase space parallel to the ΓM direction. Since the change in topology is gradual, it is difficult to see the amount of the FS nested by a particular nesting vector, but for TaS_2 and $TaSe_2$ the nesting vectors in the plane at a distance $c^*/3$ from the basal plane is close to q_{CDW}(expt.), and for $TaTe_2$ the nesting vector in $ALHAL$ plane is exactly equal to the $q_{CDW}(\text{expt.}) = 0.333a^*$. The second thing is that the magnitude of the nesting vector gradually increases on moving up from the basal plane along c axis and becomes maximum in the $ALHAL$ plane for the three compounds.

B. The supercell

The CDW is treated as a frozen phonon and a supercell is set up to represent this frozen phonon in one dimension. The CDW wave vectors are chosen such that they are around the candidate FS nesting vectors and are commensurate with the underlying lattice. Since there exist several nesting vectors of different magnitudes, three different supercells, for each compound, are considered in this work in order to simulate the CDW. The contribution of the CDW in the z direction is ignored and so the dimensions of the supercells are centered $5\sqrt{3}a\times a\times c$, noncentered $2\sqrt{3}a\times a\times c$, and centered $3\sqrt{3}a\times a\times c$. These corresponds to q_{CDW} of $0.200a^*$, $0.250a^*$, and $0.333a^*$, respectively.

As mentioned in the preceding section, the experimental commensurate CDW vector for $TaSe_2$ and TaS_2 is close to $0.277a^*$, if considered only in one dimension this also lies in between the two supercells of dimensions $2\sqrt{3}a\times a\times c$ and centered $3\sqrt{3}a\times a\times c$. In case of $TaTe_2$, the q_{CDW}(expt.) ($=q_N$ in $ALHAL$ plane) is well modeled by the centered supercell of dimensions $3\sqrt{3}a\times a\times c$. Thus all the candidate FS nesting vectors and the experimental CDW wave vectors lie in between the above-mentioned three supercells.

Further, we have not taken into account any component along c axis, although such exists experimentally. However, it is usually assumed to be a secondary effect.

All these supercells are shown in Fig. 2. The large spheres are the Ta atoms and the small spheres are the chalcogen atoms in all the figures. To study if the CDW is stabilized due to electron-phonon coupling, total-energy calculations are performed for the atomic relaxations within all these large unit cells.

C. The CDW distorted supercell

A CDW consists of a periodic variation in conduction-electron density having wave vector of magnitude q_{CDW}, which causes a static periodic distortion of the lattice with the same wave vector. From this structural distortion the CDW may be experimentally identified. Here we adopt a common view that the CDW order parameter is characterized by the Ta atomic displacement and hence the CDW amplitude is given by the magnitude of this displacement from the undistorted lattice.

The total energy as a function of displacement of the Ta atoms for all three compounds are shown in Fig. 3.

In Fig. 3(a) are shown the results for $TaTe_2$ in the supercell structures. The Ta atoms are moved rigidly and Te atoms are relaxed to minimize energy as well as forces for each displacement of Ta atoms. It can be noted that the supercells that correspond to the $q_{CDW}=0.25a^*$ and $0.20a^*$ are stable and do not go towards the CDW distorted state. However, the supercell corresponding to $q_{CDW}=0.333a^*[=q_{CDW}(\text{expt.}) = q_N(ALH)]$ is unstable towards CDW state. The lattice distortion that minimizes the total energy is 0.43 Å, this is the amplitude of the CDW. At this distortion of the Ta atoms, the maximum distortion for the Te atoms is 0.293 Å. The Te atoms relax away from the maxima and towards the node of the CDW at the same time trying to minimize the interlayer distance between the two Te-Ta-Te sandwiches along the c axis. The calculated energy gain connected to the CDW distortion is 6.91 mRy/formula unit. It is interesting to note that if the Te atoms are not relaxed for each displacement of the Ta atoms, but instead kept at undistorted positions, then the supercell is stable. On the other hand, if the Te atoms are kept fixed at the position of the stable CDW distorted state for each displacement of the Ta atoms, the structure is unstable towards the CDW state. Thus the atomic relaxations of the chalcogen atoms are essential to get the correct CDW state.

Figure 3(b) shows the total energy vs the Ta displacement for $TaSe_2$ in the supercell structures. In this case, the supercell for $q_{CDW}=0.200a^*$ is stable. The undistorted supercell corresponding to $q_{CDW}=0.333a^*$ is unstable towards the CDW distorted state. The amplitude of the CDW is 0.31 Å and the gain in energy is 1.30 mRy/formula unit. The maximum displacement of the Se atoms at the stable CDW state is 0.32 Å. The second supercell that corresponds to the CDW of wave vector $0.250a^*$ is also unstable towards the CDW distorted state. The Ta displacement is 0.22 Å with the maximum Se displacement of 0.09 Å. The energy gain in this case is slightly less, i.e., 0.92 mRy/formula unit. The calculated CDW amplitude is close to the value 0.25 Å determined by the x-ray-diffraction works[45] for $3q$ CDW. The chalcogen atoms (Se) in both the supercells relax in the same manner as the Te atoms in previous the case of $TaTe_2$.

In Fig. 3(c), similar results for TaS_2 are presented. Also here the undistorted centered supercell for $q_{CDW}=0.333a^*$ is unstable towards CDW distorted state, but the optimized amplitude of the CDW is much smaller, i.e., 0.058 Å. The corresponding stabilization energy is 0.074 mRy/formula unit. Unlike in the previous two cases, the chalcogen atoms

TABLE III. The density of states at the Fermi level for the CDW distorted state of the TaX_2 compounds in states/Ry/formula unit. The percentage decrease in the density of states at the Fermi level in the CDW distorted state relative to the undistorted state (%).

Compound	DOS at E_F (Undistorted state)	DOS at E_F (CDW distorted state)	Percentage decrease in DOS at E_F
TaS_2	19.1	17.8	7.0
$TaSe_2$	22.2	16.3	26.8
$TaTe_2$	29.0	18.2	37.2

in this case relax (maximum by 0.042 Å) towards the maxima and away from the node of the CDW. In the c direction, the S atoms relax so as to maximize the interlayer distance. The other two supercells which correspond to CDW with wave vectors $0.20a^*$ and $0.25a^*$ are stable.

In the case of $TaSe_2$ and TaS_2, the energy curve show shallow double minima, while for $TaTe_2$ it shows a single deep minima. It is clear that for all the compounds it is very important to relax the chalcogen atoms to get the correct energy and force minimum.

D. The effect of the CDW on the Fermi surface

To study the effect of the CDW on the FS, we have compared the FS of the undistorted supercell with the FS of the most stable distorted supercell. The FS cross sections of TaS_2, $TaSe_2$, and $TaTe_2$ in the undistorted supercell corresponding to $q_{CDW}=0.333a^*$ are presented in Figs. 4(a), 4(c), and 4(e), respectively. Since the supercells are centered of dimensions $3\sqrt{3}a\times a\times c$, the plane $X_0X_1X_0X_1$ is a three times folded $\Gamma MK\Gamma M$ plane in ΓM direction.

The FS of CDW distorted $TaTe_2$ is shown in Fig. 4(f). We notice that the rather complex FS sheets in Fig. 4(e) change to very simple contours in Fig. 4(f), which is also reflected in the fact that the density of states (DOS) at Fermi level reduces from 29.0 states/Ry/formula unit to 18.2 states/Ry/formula unit for the CDW distorted state (decrease of 37.2%). As can be seen a fair amount of gaping is produced in the FS due to distortion of the structure caused by the CDW. The same kind of effect is seen also in $TaSe_2$ [Figs. 4(c) and 4(d)], with a 26.80% decrease in DOS at E_F. For TaS_2 the density of states at Fermi level decreases by only 7.0% and the FS does not show any significant gaping [Figs. 4(a) and 4(b)], this could be due to very small amplitude of the CDW and that a single q CDW is not sufficient. The density of states at Fermi level for all three compounds are given in Table III.

IV. CONCLUSIONS

In the present work, in order to investigate the effect of single q commensurate CDW on the FS of group VB TMDC, $1T$-$TaX_2(X=\mathrm{S,Se,Te})$, we have treated the CDW as frozen phonons of wave vectors close to the FS nesting vector. First, it is observed that the optimization of the free lattice parameter z of the $1T$ structure is crucial for the following calculations. The FS topology simplifies dramatically. The change in the FS topology is due to the fact that the bands cutting the Fermi level are very narrow, and the FS topology is very sensitive to the finer details.

The calculated FS of $1T$-$TaSe_2$ and $1T$-$TaTe_2$ show a change in topology with variation of the vector perpendicular to the basal plane. This change in topology of the FS parallel to the basal plane was seen in old theoretical calculations of the FS of $TaSe_2$ (Ref. 25), but was discarded as an artifact of the muffin-tin approximation. For this compound there exists no experimental determination of the FS in any plane other than the basal plane. Since the $1T$-$TaTe_2$ structure is highly unstable towards $C2/m$ structure, there exists no experimental data for the FS in $1T$ phase to compare our results with. However, our calculated band structure is in very good agreement with previous LMTO-ASA calculations.[36] Our calculated band structure of $1T$-TaS_2 is consistent with the previous calculations.[24,25,31] The detailed comparison with these calculations is presented in our previous work.[46] The FS of $1T$-TaS_2 does not change topology but shows variation on going along c axis. These results are in good agreement with the estimates of the FS from 2D photoelectron images,[44] azimuthal ARPES data,[31,37] and the FS mapping experiments,[9] where the FS shows a broadening (for example Fig. 8 of Ref. 31 and Fig. 1 of Ref. 9) of the electron sheet around MA on moving up from the basal plane along the c axis.

The candidate FS nesting vectors for the three compounds are parallel to ΓM direction. The change in the FS with variation of the wave vector perpendicular to the basal plane does not change the direction of the nesting vector, but the magnitude of the nesting vector increases on moving up from the basal plane along the c axis for all the compounds. There are several possible nesting vectors of different magnitude in the phase space parallel to the ΓM direction. The change in topology is gradual and so it is difficult to see the amount of the FS nested by a particular nesting vector. However, it was noted that for TaS_2 and $TaSe_2$ the magnitude of the FS nesting vector in the plane at a distance $c^*/3$ from the basal plane is in good agreement with the CDW wave vector observed in electron-diffraction experiments. For $TaTe_2$, the calculated FS nesting vector in $ALHAL$ plane is exactly equal to CDW vector observed in the electron-diffraction experiments.

We have reproduced the lattice distortions caused by an assumed single q commensurate CDW in these compounds by moving the Ta atoms rigidly and relaxing the chalcogen atoms, to minimize energy as well as forces for each displacement of Ta atoms. The distortions caused by three

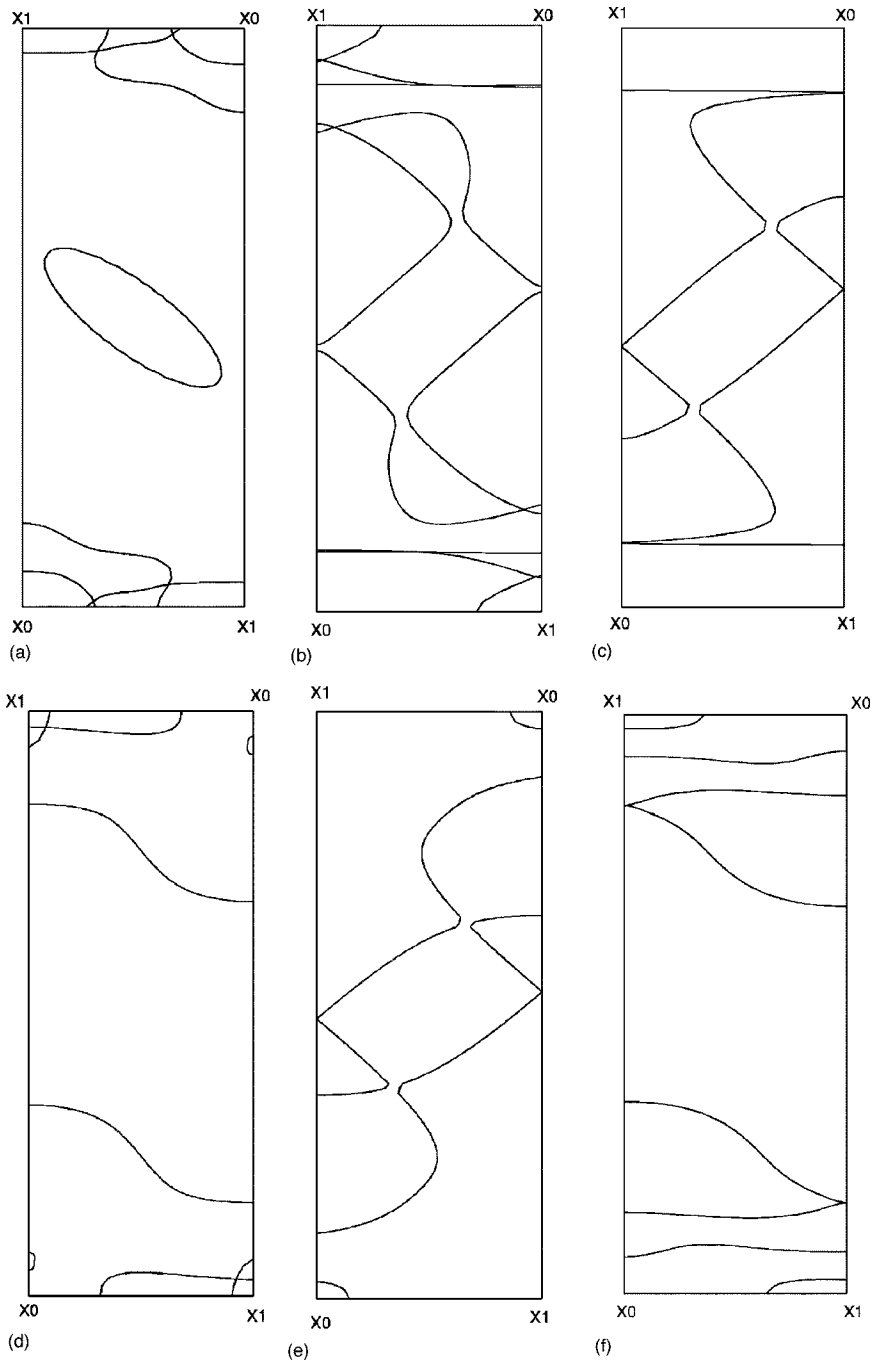

FIG. 4. (a) The Fermi-surface cross section of TaS_2 in the undistorted supercell structure corresponding to $q_{CDW}=0.333a^*$. (b) The Fermi-surface cross section of TaS_2 in the supercell structure distorted by the CDW of wave vector $q_{CDW}=0.333a^*$ and amplitude 0.058 Å. (c) The Fermi-surface cross section of $TaSe_2$ in the undistorted supercell structure corresponding to $q_{CDW}=0.333a^*$. (d) The Fermi-surface cross section of $TaSe_2$ in the supercell structure distorted by the CDW of wave vector $q_{CDW}=0.333a^*$ and amplitude 0.31 Å. (e) The Fermi-surface cross section of $TaTe_2$ in the undistorted supercell structure corresponding to $q_{CDW}=0.333a^*$. (f) The Fermi-surface cross section of $TaTe_2$ in the supercell structure distorted by the CDW of wave vector $q_{CDW}=0.333a^*$ and amplitude 0.43 Å.

CDW's of wave vectors $0.200a^*$, $0.250a^*$, and $0.333a^*$, respectively, were studied and it was found that the three compounds studied in this work are unstable towards the state distorted by the CDW of wave vector $0.333a^*$. The energy gain connected to the CDW distortion is maximum for $TaTe_2$ and minimum for TaS_2. Same is true for the amplitude of the CDW, which is maximum for $TaTe_2$ and minimum for TaS_2. It was shown that the relaxation of the chalcogen atoms is essential to reproduce a stable distorted structure. The chalcogen atoms in $TaTe_2$ and $TaSe_2$ always relax away from the CDW maxima and at the same time trying to minimize the interlayer distance between X-Ta-X sandwiches. While for TaS_2 the S atoms follow the Ta atoms and relax towards the CDW maxima.

Our FS calculations for the CDW distorted structure confirm the presence of gaping in the FS for $TaSe_2$ and $TaTe_2$ caused by the CDW's. Since the FS is only partially gaped, the system retains metallic character even in the CDW state, but the DOS at Fermi level reduces compared to the undistorted structure. In the case of TaS_2, the FS of CDW distorted state does not show any significant gaping and the DOS at Fermi level decreases by 7.0%, which is very small compared to $TaTe_2$ where this decrease is 37.2% or $TaSe_2$ where it is 26.8%. This could be due to the amplitude of the CDW being very small and the single q CDW alone is not sufficient to produce any kind of gapping in the FS and it is essential to study the $3q$ CDW.

The present investigation shows that the FS for the compounds under investigation shows gradual change in topology in the phase space, and it is very difficult to determine the exact nesting vector that spans maximum portion of the FS. The study of the single q commensurate CDW treated as a frozen phonon show that electron-phonon coupling can stabilize CDW in the $1T$-TaX_2 systems. These CDW distortions produce gaping in the FS and decrease the DOS at the Fermi level. The effect of the FS nesting on the CDW stabilization is strong and cannot be ignored. The distortion effect of commensurate $3q$ CDW could be to produce a complete gaping in the FS. However, the study of this kind requires enormous amount of computer time and memory and is the subject of future investigation.

ACKNOWLEDGMENTS

We would like to acknowledge the Swedish Research Council (VR) for the financial support and Swedish National Supercomputer Center in Linköping (NSC) for the use of their computational facilities. We would also like to thank A. Taga and E. Sjöstedt for comments and suggestions.

[1] C.M. Fang, R.A. de Groot, and C. Haas, Phys. Rev. B **56**, 4455 (1997).
[2] Albert Spijkerman, J.L. de Boer, Auke Meetsma, G.A. Wiegers, and S.V. Smaalen, Phys. Rev. B **56**, 13 757 (1997).
[3] Jens Lüdecke, Edmund Riedl, Mathias Dierl, Khalil Hosseini, and Sander van Smaalen, Phys. Rev. B **62**, 7057 (2000).
[4] Akiji Yamamoto, Phys. Rev. B **27**, 7823 (1983).
[5] M.D. Núñez-Regueiro, J.M. Lopez-Castillio, and C. Ayache, Phys. Rev. Lett. **55**, 1931 (1985).
[6] N.V. Smith and M.M. Traum, Phys. Rev. B **11**, 2087 (1975).
[7] N.V. Smith, S.D. Kevan, and F.J. DiSalvo J. Phys. C **18**, 3175 (1985).
[8] R. Claessen, B. Burandt, H. Carstensen, and M. Skibowski, Phys. Rev. B **41**, 8270 (1990).
[9] Th. Pillo, J. Hayoz, H. Berger, M. Grioni, L. Schlapbach, and P. Aebi, Phys. Rev. Lett. **83**, 3494 (1999).
[10] Kanta Ono Koji Horiba, Han Woong Yeom, Yoshihiro Aiura, Osamu Shiino, Jin Ho Oh, and Takayuki Kihara, Physica B **284**, 1665 (2000).
[11] S. Hüfner, R. Claessen, F. Reinert, Th. Straub, V.N. Strocov, and P. Steiner, J. Electron Spectrosc. Relat. Phenom. **100**, 191 (1999).
[12] B. Darel, M. Grioni, D. Malterre, P. Wiebel, and Y. Baer, Phys. Rev. B **45**, 1462 (1992).
[13] M.M. Traum, N.V. Smith, and F.J. DiSalvo, Phys. Rev. Lett. **32**, 1241 (1974).
[14] M. Eibschutz, Phys. Rev. B **45**, 10 914 (1992).
[15] F.J. DiSalvo, J.A. Wilson, B.G. Bageley, and J.V. Waszczak, Phys. Rev. B **12**, 2220 (1975).
[16] H. Bando, K. Koizumi, Y. Miyahara, and H. Ozaki, J. Phys.: Condens. Matter **12**, 4353 (2000).
[17] J.A. Wilson, F.J. Disalvo, and S. Mahajan, Adv. Phys. **24**, 117 (1975).
[18] H.J. Crawack, Y. Tomm, and C. Pettenkofer, Surf. Sci. **465**, 301 (2000).
[19] B. Giambattista, C.G. Slough, W.W. McNairy, and R.V. Coleman, Phys. Rev. B **41**, 10 082 (1990).
[20] B. Burk, R.E. Thomson, A. Zettl, and John Clarke, Phys. Rev. Lett. **66**, 3040 (1991).
[21] Ju-Jin Kim, Chan Park, W. Yamaguchi, O. Shiino, K. Kitazawa, and T. Hasegawa, Phys. Rev. B **56**, 15 573 (1997).
[22] J.A. Wilson and A.D. Yoffe, Adv. Phys. **18**, 193 (1969).
[23] R.A. Bromley, R.B. Murray, and A.D. Yoffe, J. Phys. C **5**, 759 (1972).
[24] L.F. Mattheiss, Phys. Rev. B **8**, 3719 (1973).
[25] H.M. Myron and A.J. Freeman, Phys. Rev. B **11**, 2735 (1975).
[26] A. Vernes, H. Ebert, W. Bensch, W. Heid, and C. Näther, J. Phys.: Condens. Matter **10**, 761 (1998).
[27] Sangeeta Sharma, S. Auluck, and M.A. Khan, Pramana, J. Phys. **54**, 431 (2000).
[28] J.A. Wilson, F.J. DiSalvo, and S. Mahajan, Phys. Rev. Lett. **32**, 882 (1974).
[29] P. Fazekas and E. Tosatti, Philos. Mag. B **39**, 229 (1979).
[30] K. Okajima and S. Tanaka, J. Phys. Soc. Jpn. **53**, 2332 (1984).
[31] Th. Pillo, J. Hayoz, H. Berger, R. Fasel, L. Schlapbach, and P. Aebi, Phys. Rev. B **62**, 4277 (2000).
[32] F.J. DiSalvo, J.A. Wilson, and J.V. Waszczak, Phys. Rev. Lett. **36**, 885 (1976).
[33] F.J. Disalvo and J.E. Graebner, Solid State Commun. **23**, 825 (1977).
[34] H. Fukuyama and K. Yosida, J. Phys. Soc. Jpn. **46**, 102 (1976).
[35] H. Fukuyama and K. Yosida, J. Phys. Soc. Jpn. **46**, 1522 (1976).
[36] M-L. Doublet, S. Remy, and F. Lemingo, J. Chem. Phys. **113**, 5879 (2000).
[37] P. Aebi, Th. Pillo, H. Berger, and F. Lévy, J. Electron Spectrosc. Relat. Phenom. **117**, 433 (2001).
[38] G. Santoro, S. Scandolo, and E. Tosatti, Phys. Rev. B **59**, 1891 (1999).
[39] A.P. Baddorf, V. Jahns, Jiandi Zhang, J.M. Carpinelli, and E.W. Plummer, Phys. Rev. B **57**, 4579 (1998).
[40] T.E. Kidd, T. Miller, and T.C. Chiang, Phys. Rev. Lett. **83**, 2789 (1999).
[41] A. Goldoni and D. Modesti, Phys. Rev. Lett. **79**, 3266 (1997).
[42] T. Yokoya, T. Kiss, A. Chainani, S. Shin, M. Nohara, and H.

Takagi, Science **294**, 2518 (2001).
[43] P. Blaha, K. Schwarz, P. Sorantin, and S.B. Trickey, Comput. Phys. Commun. **59**, 399 (1990).
[44] R.A. Pollak, D.E. Eastman, F.J. Himpsel, and B. Reihl, Phys. Rev. B **24**, 7435 (1981).
[45] R. Brouwers and F. Jellinek (unpublished).
[46] Sangeeta Sharma, Ph.D. dissertation, University of Roorkee, 1999.